Published in final edited form as:

Biochim Biophys Acta. 2017 August ; 1863(8): 1870–1882. doi:10.1016/j.bbadis.2016.10.003.

Cardiomyocyte-specific deletion of the G protein-coupled estrogen receptor (GPER) leads to left ventricular dysfunction and adverse remodeling: a sex-specific gene profiling analysis

Hao Wang[a,b], **Xuming Sun**[a], **Jeff Chou**[c], **Marina Lin**[a], **Carlos M. Ferrario**[d,e], **Gisele Zapata-Sudo**[a,f], and **Leanne Groban**[a,b,g,h]

[a]Department of Anesthesiology, Wake Forest School of Medicine, Medical Center Blvd., Winston-Salem, NC 27157-1009 USA

[b]Internal Medicine/Molecular Medicine, Wake Forest School of Medicine, Medical Center Blvd., Winston-Salem, NC 27157 USA

[c]Public Health Sciences, Section on Biostatistical Sciences, Wake Forest School of Medicine, Medical Center Blvd., Winston-Salem, NC 27157 USA

[d]Department of Surgery, Wake Forest School of Medicine, Medical Center Blvd., Winston-Salem, NC 27157 USA

[e]Department of Internal Medicine/Nephrology, Wake Forest School of Medicine, Medical Center Blvd., Winston-Salem, NC 27157 USA

[f]Institute of Biomedical Sciences, Drug Development Program, Federal University of Rio de Janeiro, Brazil

[g]Cardiovascular Research Center, Wake Forest School of Medicine, Medical Center Blvd., Winston-Salem, NC 27157 USA

[h]Sticht Center on Aging, Wake Forest School of Medicine, Medical Center Blvd., Winston-Salem, North Carolina, 27157 USA

Abstract

Activation of G protein-coupled estrogen receptor (GPER) by its agonist, G1, protects the heart from stressors such as pressure-overload, ischemia, a high-salt diet, estrogen loss, and aging, in various male and female animal models. Due to nonspecific effects of G1, the exact functions of cardiac GPER cannot be concluded from studies using systemic G1 administration. Moreover, global knockdown of GPER affects glucose homeostasis, blood pressure, and many other cardiovascular-related systems, thereby confounding interpretation of its direct cardiac actions. We

Address correspondence to: Hao Wang, MD, PhD, Department of Anesthesiology, Wake Forest School of Medicine, Medical Center Boulevard, Winston-Salem, NC 27157-1009, Phone: 336-713-9171, Fax: 336-716-8190, haowang@wakehealth.edu**Or** Leanne Groban, MD, Department of Anesthesiology, Wake Forest School of Medicine, Medical Center Boulevard, Winston-Salem, NC 27157-1009, Phone: 336-716-4498, Fax: 336-716-8190, lgroban@wakehealth.edu.

generated a cardiomyocyte-specific GPER knockout (KO) mouse model to specifically investigate the functions of GPER in cardiomyocytes. Compared to wild type mice, cardiomyocyte-specific GPER KO mice exhibited adverse alterations in cardiac structure and impaired systolic and diastolic function, as measured by echocardiography. Gene deletion effects on left ventricular dimensions were more profound in male KO mice compared to female KO mice. Analysis of DNA microarray data from isolated cardiomyocytes of wild type and KO mice revealed sex-based differences in gene expression profiles affecting multiple transcriptional networks. Gene Set Enrichment Analysis (GSEA) revealed that mitochondrial genes are enriched in GPER KO females, whereas inflammatory response genes are enriched in GPER KO males, compared to their wild type counterparts of the same sex. The cardiomyocyte-specific GPER KO mouse model provides us with a powerful tool to study the functions of GPER in cardiomyocytes. The gene expression profiles of the GPER KO mice provide foundational information for further study of the mechanisms underlying sex-specific cardioprotection by GPER.

Keywords

GPER; knockout; cardiomyocyte; microarray

1. Introduction

Cardiovascular disease (CVD) remains the leading cause of death in women in the United States, accounting for almost 400 million female deaths in 2013 [1]. The CVD morbidity rate in premenopausal women is lower compared with age-matched men, while the rate exceeds that of men after menopause [2,3]. The female sex hormone estrogen is thought to contribute to the observed differences in CVD morbidity between men and women and between pre- and postmenopausal women [2,4]. However, there is no clear evidence of an association between estrogen-based hormone replacement therapy and lower rates of cardiovascular outcomes or all-cause mortality in the postmenopausal population [5]. Rather, the available evidence shows that the risk of CVD, as well as breast cancer, increases with estrogen-based hormone therapy [5–8]. A better understanding of the relationship between estrogen and CVD risk in postmenopausal women, as well as the mechanisms and specific receptors that drive the estrogen effect, is needed to inform the development of specific cardioprotective treatments with fewer side effects.

The G protein-coupled estrogen receptor (GPER), also called GPR30, is an estrogen receptor (ER) that is expressed in the heart. GPER was first cloned from human B-cell lymphoblasts in 1996 [9], and in the intervening decade, several studies have demonstrated that activation of GPER protects the heart from various stresses such as pressure-overload, ischemia, a high-salt diet, estrogen loss, and aging in both male and female animal models [10–13]. Both *in vivo* and *in vitro* studies have examined the cardioprotective effects of GPER activated by its agonist, G1; however, G1 also binds and activates ERα36 and has nonspecific cardiac effects that confound analysis of GPER function [14]. A whole-body GPER knockout (KO) mouse has also been generated, though global elimination of GPER was shown to influence glucose homeostasis and blood pressure via various actions on smooth muscle cells, endothelial cells, fibroblasts, and cardiac mast cells [15–21].

To determine the specific function of GPER in cardiomyocytes, we generated a cardiomyocyte-specific GPER KO mouse. We compared basal cardiac function and structure, systemic blood pressure, and exercise tolerance in male and female wild type (WT) and cardiomyocyte-specific GPER KO mice and performed DNA microarray analysis to identify differential gene expression profiles and transcriptional networks. We hypothesize that GPER deletion in cardiomyocytes induces the morphometric impairments and functional declines in the heart of both sexes compared to their intact counterparts. The microarray data from GPER KO vs. intact cardiomyocytes would be important for future studies on the exact roles of GPER in the heart and the underlying mechanisms of sex-specific cardioprotection.

2.0 Materials and Methods

All mice were housed in a facility approved by the Association for Assessment and Accreditation of Laboratory Animal Care with a 12-h light/dark cycle and constant temperature and humidity. Mice had *ad libitum* access to standard chow (Nestle Purina, St. Louis, MO) and tap water. All procedures were in performed in compliance with the *Guide for the Care and Use of Laboratory Animals*, published by the National Institutes of Health, and were reviewed and approved by the Wake Forest School of Medicine's Animal Care and Use Committee before commencement of the study (Approved protocol #A13-178).

2.1. Generation of cardiomyocyte-specific GPER KO mice

An embryonic stem (ES) cell clone (EPD0334_2_H06) carrying a GPER KO allele with conditional potential ($GPER^{tm1a(KOMP)Wtsi}$) and flanking loxP sites within exon 3 was generated, expanded, and injected into C57BL/6 blastocysts as part of the Knockout Mouse Project (KOMP), as previously described [22] (Figure 1). Germ-line transmission was achieved by mating male chimeric founders with C57BL/6N female mice. The C57BL/6N mouse harboring a first mutation KO at the GPER locus was crossed with a Flp recombinase deleter mouse, C57BL/6N-Tg(CAG-Flpo)1Afst/Mmucd (Mutant Mouse Regional Resource Center, University of California, Davis, CA), to remove the selection cassette and generate a GPER allele with a floxed region in exon 3, which is the only coding exon of the GPER gene. Cardiomyocyte-specific GPER KO mice ($GPER^{f/f/Cre}$) were generated by crossing homozygous GPER-floxed animals ($GPER^{f/f}$) with transgenic mice expressing Myh6-Cre recombinase under the control of the cardiomyocyte-specific α myosin-heavy chain 6 promoter (Myh6) (The Jackson Laboratory, Bar Harbor, ME). Genotyping of the GPER floxed allele was performed using PCR with primers 1 (5′-GAA CCC ACA GCT CTC TTG TGT GC-3′) and 2 (5′-GAG TGT GTG GTG TGG GAA TTT GAG G-3′), which amplified a 530-bp fragment, whereas the GPER WT allele produced a 345-bp fragment. The α-Myh6-Cre transgene was detected by PCR using the primers 5′-ATG ACA GAC AGA TCC CTC CTA TCT CC-3′ and 5′-CTC ATC ACT CGT TGC ATC ATC GAC-3′, which amplified a 300-bp fragment.

2.2. Blood pressure (BP) measurement

Systolic blood pressure (SBP) was measured noninvasively using a volume-pressure recording tail-cuff method on conscious, restrained mice using the CODA 6 system (Kent

Scientific Corp, Torrington, CT). Briefly, mice were gently placed in the restrainer and allowed to rest quietly for 10 min at 30°C prior to obtaining 5 acclimation cycles followed by 10 measurement cycles. SBP measurements were collected and averaged. All measurements were performed between 9:00–11:00 a.m. for all groups, to account for any diurnal variations.

2.3. Exercise capacity test

The maximal exercise capacity test (time to exhaustion during a standardized exercise protocol) was performed using a motorized treadmill (Scientific Instruments, Stoelting, Wood Dale, IL). Mice were familiarized with the motor-driven, one-lane rodent treadmill by walking at a speed of 20 cm/s, 10 min/d, for 1 week. Each exercise test was performed after at least 1 day of rest. The protocol for exercise capacity evaluation consisted of 3 min at 12 meters/min, with 1.2-meter/min increases in speed every 3 min until the mouse reached exhaustion. Time to exhaustion (in min) was determined when the mouse was unable to continue running and sat at the lower end of the treadmill for more than 5 s, despite gentle nudging.

2.4. Echocardiography

Left ventricular (LV) structure and function were determined in 15-week-old male and female cardiomyocyte-specific GPER KO mice ($GPER^{f/f/Cre}$ and WT mice ($GPER^{f/f}$) using a commercially available echocardiograph equipped with both PureWave 12-4 MHz sector and 15-7 MHz linear transducers (CX50 CompactXtreme System; Philips Medical Systems) by the same investigator (L.G.), who was blinded to the experimental groups as previously described [23]. In brief, mice were anesthetized with an isoflurane (1.5%) oxygen mixture by nose cone and secured in the supine position to a warm (37.5°C) imaging platform. A 15 MHz linear probe was used to obtain 2D-guided, LV M-mode images using parasternal long and short axis views for measures of LV end diastolic and end systolic dimensions (LVEDD and LVESD) and posterior and anterior wall thicknesses (PWTed and AWTed) at end diastole. A 12 MHz phased array probe was used to obtain the apical 4-chamber view for transmitral inflow Doppler (early transmitral filling or maximum E-wave velocity) and septal tissue Doppler measurements (early mitral annular descent or e′) of diastolic function. Heart rate was determined from five consecutive RR intervals from pulsed-Doppler inflow tracings. The fractional shortening (FS) of the LV was expressed as %FS = (LVEDD-LVESD)/LVEDD × 100. The relative wall thickness (RWT) was calculated as (PWTed + AWTed)/LVEDD. The early mitral inflow filling velocity-to-early mitral annular descent velocity ratio, or E/e′, was used to estimate LV filling pressure. E/e′ is a useful measure to assess the severity of LV stiffness or diastolic dysfunction.

2.5. Cardiomyocyte isolation

Mice at 18–20 weeks of age were injected i.p. with 200 μl heparin (Sagent Pharmaceutical Inc., Schaumburg, IL, 100 IU/mouse) 10 min prior to anesthesia with pentobarbital (Akorn Inc., Lake Forest, IL, 100 mg/kg body weight) by i.p. injection. Upon verification of deep anesthesia by the absence of response to tail/toe pinches, the heart was quickly removed and trimmed in an ice-cold, calcium-free perfusion buffer (126 mM NaCl, 4.4 mM KCl, 1 mM $MgCl_2$, 4 mM NaHCO3, 10 mM HEPES, 11 mM glucose, 30 mM 2,3-butanedine

monoxime [Sigma, St. Louis, MO], 5 mM taurine [Sigma], pH 7.35). The heart was then cannulated through the aorta on an Easycell System for Cardiomyocyte Isolation (Harvard Apparatus, Holliston, MA) and perfused at 37°C with calcium-free perfusion buffer at a flow rate of 3 ml/min for 4–5 min until the effluent became clear. The heart was switched to digestion buffer (perfusion buffer plus 50 μM $CaCl_2$ and 0.5 mg/ml collagenase II [Worthington Biochemical Corp., Freehold, NJ]), and perfused for 10–15 min at a flow rate of 4 ml/min until the heart was pale and flaccid. The heart was pulled from the cannula and the ventricles were transferred to a 60-mm sterile dish containing 5 ml of transfer buffer (perfusion buffer plus 0.1 mM $CaCl_2$ and 2% bovine serum albumin [Sigma]) and cut into small pieces. The minced tissue was incubated in a 37°C water bath for 10 min. The cell suspension was filtered through a 100-μm mesh cell strainer (BD Biosciences, San Jose, CA) to remove tissue debris and spun at 420 rpm at room temperature for 2 min. After removing the supernatant, the cardiomyocytes were washed with 1 ml of PBS and centrifuged at 1500 rpm at 4°C for 3 min. The cells were suspended in 1 ml of QIAzol (Qiagen Inc, Valencia, CA), mixed, and homogenized before storing at −80°C.

2.6. DNA microarray assay

Total RNA was isolated from cardiomyocytes using the RNeasy Lipit Tissue Mini Kit (Qiagen Inc) and further purified using RNeasy MinElute Cleanup Kit (Qiagen Inc) followed by quality assessment on an Agilent 2100 bioanalyzer. Samples with RIN values >8.0 and a 260/280 ratio between 1.8 and 2.1 were carried forward for cRNA synthesis and hybridization to GeneAtlas MG-430 PM Array Strips (Affymetrix, Santa Clara, CA) following the manufacturer's recommended protocol. Briefly, approximately 250 ng of purified total RNA was reverse transcribed and biotin labeled to produce biotinylated cRNA targets according to the standard Affymetrix GeneAtlas 3'-IVT Express labeling protocol (GeneAtlas 3' IVT Expression Kit User Manual, P/N 702833 Rev. 4, Affymetrix). Following fragmentation, 6 μg of biotinylated cRNA was hybridized for 16 h at 45°C on the Affymetrix GeneAtlas Mouse MG-430 PM Array Strip. Strips were washed and stained using the GeneAtlas Fluidics Station according to standard Affymetrix operating procedures (GeneAtlas™ System User's Guide, P/N 08-0306 Rev. A January 2010). Strips were subsequently scanned using the GeneAtlas Imager system according to the standard Affymetrix protocol. Fluidics control, scan control, and data collection were performed using the GeneAtlas Instrument Control Software version 1.0.5.267. All microarray analyses were performed by the Wake Forest School of Medicine Microarray Shared Resource Core.

2.7. Microarray data analysis

Gene expression profiles of cardiomyocytes detected by DNA microarray were estimated by RMA normalization and log2 converted probe set pixel intensity [24]. Paired analysis of differentially expressed genes between cardiomyocyte-specific GPER KO and WT cardiomyocytes from male and female mice were identified by Empirical Bayes method [25] implemented in the R Biocondoctor limma package, where the selection thresholds used were logFC (fold change) >1 and FDR (False Discovery rate) $P<0.01$.

EPIG (Extracting Patterns and Identifying differentially expressed Genes) analysis [26] was employed to evaluate gene expression data from WT and cardiomyocyte-specific GPER KO

male and female mice. EPIG uses an un-supervised profile approach to extract patterns from the whole data set and then categorize genes to one of the patterns if they met all the following criteria: signal/noise ratio (SNR) >3 (i.e., the corresponding *P*-value is <0.05), fold change >1, and the maximum Pearson correlation *r* value to a given pattern of >0.64.

2.8. Ingenuity pathway analysis (IPA) and Gene set enrichment analysis (GSEA)

Functional annotation to gene ontology was performed using IPA software (Ingenuity Systems, Inc., Redwood City, CA). GSEA was performed to determine whether genes belonging to a biological pathway or a previously determined functional group were significantly overrepresented at the top or bottom of a ranked gene list compared to controls without a predefined cut-off value. This bioinformatic tool evaluates all significantly measured targets derived from a microarray experiment at the level of gene sets, which are defined based on prior biological knowledge. Thus, biologically relevant information is not missed by losing target genes due to an “arbitrarily” chosen cut-off value. In this study, expression data of all 21,782 genes were compared against functional gene sets to determine whether any of these sets were enriched in GPER KO cardiomyocytes vs. WT cardiomyocytes.

2.9. RT-PCR

Total RNA was extracted from tissues (brain, lung, liver, spleen, aorta, diaphragm, kidney, stomach, small intestine, skeletal muscle, and fat) or cardiomyocytes, and purified and qualified as described above for the microarray assay. Complimentary first strand DNA was synthesized from oligo (dT) primed total RNA using the Omniscript RT kit (Qiagen Inc). PCR amplification of GPER and the housekeeping gene glyceraldehyde-3-phosphate dehydrogenase (GAPDH) were performed under the following PCR conditions: initial denaturation at 95°C for 10 min, followed by 30 cycles of 94°C for 30 s, 60°C for 30 s, and 72°C for 30 s. The size of the amplified GPER product was 172 bp and GAPDH was 110 bp. PCR products were visualized on 1% agarose gel (Sigma) stained with ethidium bromide and observed under ultraviolet light.

2.10. Real-time quantitative PCR

Relative quantification of mRNA levels by real-time qPCR was performed using a SYBR Green PCR kit (Qiagen Inc), as previously described [11]. Amplification and detection were performed with the ABI7500 Sequence Detection System (Applied Biosystems, Foster City, CA). Sequence-specific oligonucleotide primers were designed according to published GenBank sequences and confirmed with OligoAnalyzer 3.0. The primer sequences are listed in the supplemental table. The relative target mRNA levels in each sample were normalized to GAPDH. Expression levels are reported relative to the geometric mean of the control group.

2.11. Statistical analyses

For all experiments except the microarray analysis, values are reported as mean ± SEM. Two-way ANOVA was used to determine the effect of GPER status (KO vs. WT) and sex (male vs. female), followed by Tukey’s multiple comparisons test. Data were analyzed using

the software GraphPad Prism Version 6 (GraphPad Software, Inc., La Jolla, CA). Differences for all tests were considered significant at $P<0.05$.

3.0 Results

3.1. Confirmation of GPER KO specifically in cardiomyocytes

Figure 1B is a representative image of the genotyping results for homozygous and heterozygous loxP-flanked GPER ($GPER^{f/f}$) mice and WT GPER mice. The mice grew normally into adulthood without any health problems. Figure 1C shows a representative image of genotyping results for the Cre transgenic mice. RT-PCR confirmed a significant knockdown of GPER expression in cardiomyocytes isolated from GPERf/f/Cre mice (KO) compared with $GPER^{f/f}$ mice (WT) (Figure 1D). GPER expression in other tissues (brain, lung, liver, spleen, aorta, diaphragm, kidney, stomach, small intestine, skeletal muscle, and fat) was not different between the GPER KO and WT mice (Figure 1E).

Expression of ERα and ERβ was also determined by real-time RT-qPCR. As shown in Table 1, knockdown of GPER in the cardiomyocytes did not affect ERα or ERβ mRNA levels in cardiomyocytes in either male or female mice.

3.2. Body weight, blood pressure, and exercise capacity

Body weight, blood pressure, and exercise tolerance characteristics are shown in Table 1. Body weight was significantly higher in male vs. female mice [sex effect: $F(1,17) = 86.4$, $P<0.0001$], irrespective of GPER deletion in cardiomyocytes [KO effect: $F(1,17) = 3.79$, $P=0.068$]. There were no effects of sex or GPER deletion on systolic blood pressure. While exercise tolerance, as measured by treadmill stress test, was greater in female mice vs. male mice [sex effect: $F(1,17) = 41.9$, $P<0.0001$], GPER deletion in cardiomyocytes did not influence physical performance [KO effect: $F(1,17) = 0.25$, $P=0.624$].

3.3. Heart structure and function

Echocardiographic indices of LV dimensions, wall thickness, and systolic and diastolic function are shown in Figure 2. Heart rates under isoflurane anesthesia were not significantly different between sexes (481 ± 22 and 401 ± 21 beats/min in WT males and females, respectively) [sex effect: $F(1,18) = 2.24$, 0.299], and the deletion of GPER in cardiomyocytes did not influence this variable [KO effect $F(1,18) = .77$, 0.39]. There was a significant interaction between sex and KO [sex × KO effect: $F(1,18) = 7.51$, $P=0.014$]; heart rate dropped by 15% in male rats with cardiomyocyte-specific deletion of GPER, whereas it increased by 8% in females. LVESD exhibited a marked increase in cardiomyocyte-specific GPER KO mice compared to WT mice [KO effect: $F(1,18) = 11.58$, $P=0.003$], and this effect was more profound among the males [sex × KO effect: $F(1, 18) = 6.295$, $P=0.022$]. For LVEDD and RWT, there were no overt sex or cardiomyocyte-specific GPER deletion effects. Nonetheless, among males, GPER deletion increased LVEDD by 13% compared to WT mice, whereas in females, this LV dimension was not affected by gene deletion [sex × KO effect: $F(1,18) = 4.99$, $P=0.038$]. An interaction effect between sex and cardiomyocyte-specific GPER deletion was also observed for RWT [sex × KO effect: $F(1,18) = 4.34$, $P=0.052$]. Specifically, among males, deletion of GPER in cardiomyocytes had a wall-

thinning effect compared to WT males, whereas among females, GPER knockdown in cardiomyocytes had an overall wall-thickening effect compared to WT females. Global systolic function was affected by sex and deletion of GPER in cardiomyocytes, as the %FS was lower in both females vs. males [sex effect: $F(1,18) = 8.47$, $P=0.009$) and in the GPER KO vs. WT mice [KO effect: $F(1,18) = 20.42$, $P=0.0003$]. The tissue Doppler measure of myocardial relaxation, mitral annular descent (e') was also significantly affected by both sex and GPER deletion. Specifically, e' was lower in female vs. male mice [sex effect: $F(1,17) = 4.99$, $P=0.039$], and in cardiomyocyte-specific GPER KO vs. WT mice [KO effect: $F(1,17) = 20.49$, $P=0.0003$). The effect of GPER deletion on this parameter of diastolic function appeared to be more profound in males than in females [sex × KO effect: $F(1,17) = 4.37$, $P=0.052$]. Although there were no sex differences in LV filling pressures (E/e'), there was a significant effect of cardiomyocyte-specific GPER KO [$F(1,17) = 16.74$, $P=0.0008$], particularly between female KO and female WT mice ($P<0.05$).

Atrial natriuretic factor (ANF) and brain natriuretic peptide (BNP) are biomarkers for cardiac hypertrophy and heart failure. Consistent with the echocardiographic findings, results from real-time qPCR showed that ANF and BNP levels in cardiomyocytes were significantly higher in cardiomyocyte-specific GPER KO mice compared with WT mice, irrespective of sex (ANF, KO effect: $F(1,12) = 117.6$, $P<0.0001$; BNP, $F(1,12) = 8.203$, $P=0.014$] (Table 1).

3.4. DNA microarray paired analysis results from isolated cardiomyocytes

45,141 probe sets in the DNA microarray assay detected 21,781 genes, with some probe sets corresponding to the same Entrez Gene ID. The gene expression changes in GPER KO vs. WT cardiomyocytes were different between female and male mice. Tables 2–5 list the top 50 most significantly upregulated and downregulated genes in cardiomyocytes of female and male cardiomyocyte-specific GPER KO vs. WT mice. Some genes, including ANF and BNP (Table 1), were selected for verification by real-time qPCR.

3.5. EPIG analysis based on sex and GPER expression

278 probes were found to be significantly responsive to the cardiomyocyte-specific knockout of GPER from male and female mice and categorized into eight different patterns, as summarized in Figure 3. Similar gene expression patterns between GPER KO and their WT female and male counterparts are displayed in panels 3D and 3H, while the other panels illustrate gene expression patterns with marked differences respect to sex and cardiomyocyte-specific GPER deletion. The names of the genes in each panel are available upon request.

3.6. Pathway analysis

To examine the differences in the mitochondrial and inflammatory response gene expressions between GPER KO and WT cardiomyocytes, microarray data were loaded into GSEA 2.0.1 using GSEA gene sets “MITOCHONDRION (including 314 genes)” and “HALLMARK_INFLAMMATORY_RESPONSE (including 193 genes).” The results showed that the mitochondrial genes were enriched in GPER-KO vs. WT cardiomyocytes from female, but not male, mice. In contrast, the inflammatory response genes were enriched

in GPER KO vs. WT cardiomyocytes from male, but not female, mice (Figure 4). The heat maps and the individual mitochondrial and inflammatory gene changes in GPER knockout versus intact cardiomyocytes from both sexes are presented in Data In Brief [27].

IPA revealed differences in canonical pathways and genes related to various diseases and disorders, molecular and cellular functions, physiological system development and functions, and cardiotoxicity between GPER KO vs. WT cardiomyocytes of male and female mice (Tables 6 and 7).

3.7. Cardiac hypertrophy-related gene expression

Although LV hypertrophy was not overtly apparent *in vivo* in the hearts of cardiomyocyte-specific GPER KO mice compared to WT mice (Table 1), IPA revealed significant sex-specific differences in cardiac hypertrophy-related gene expression between GPER KO and WT cardiomyocytes (Figure 5). Specifically, in female mice, the hypertrophy-related genes that were elevated in GPER KO vs. WT cardiomyocytes included ANKRD1, BCL-2, BMPR2, CTGF, ERBB2IP, GDF15, HIF1A, MYH7, NPPA, NT5E, POSTN, PTEN, TIMP1, and TLR4; while PFKFB1 was lower. In male mice, the hypertrophy-related genes that were elevated in GPER KO vs. WT cardiomyocytes included ANKRD1, APOE, CDKN1A, CTGF, GDF15, GPX3, MYH7, NPPA, NT5E, RCAN1, TIMP1, and TLN1; while DMD, FLT1, KCND2, PFKFB1, and PIK3R1 were lower (Figure 5).

4.0 Discussion

The present study is the first to describe the successful generation of a cardiomyocyte-specific GPER KO mouse. Compared to WT mice, echocardiography revealed the presence of adverse alterations in cardiac structure and impairments in systolic and diastolic function in cardiomyocyte-specific GPER KO mice of both sexes, with more profound increases in LV dimensions among male KO mice. Analysis of DNA microarray data from cardiomyocytes of GPER KO and WT mice showed differential expression profiles of genes affecting multiple transcriptional networks between male and female mice after cardiomyocyte-specific GPER deletion. GSEA revealed that mitochondrial genes were enriched in GPER-KO cardiomyocytes from females compared to WT males, while inflammatory response genes were enriched in GPER-KO cardiomyocytes from males compared to WT females. Taken together, our findings provide strong evidence confirming the cardioprotective effect of GPER that had been suggested by previous studies of non-specific activation of GPER with G1 and global GPER knockout techniques.

The discovery of GPER, especially its expression in the heart, has opened up a new direction for research into the cardioprotective effects of estrogen and the mechanisms underlying CVD risk in older women after the loss of ovarian estrogen function. Studies in animal models using an agonist of GPER, G1, have shown that both chronic and acute treatment with G1 limits LV dysfunction and improves cardiac remodeling induced by ischemia/reperfusion, hypertension, high-salt diet, or estrogen loss [10,11,13,28–31]. In male global GPER knockout mice, the LV is enlarged and LV contractility and relaxation capacities are reduced [32]. Despite these examples of GPER-mediated cardioprotection, the exact roles of cardiac GPER could not be concluded, as the specificity of G1 binding to GPER is

questionable [14]. The systemic administration of G1 or global GPER knockout also have effects on other tissues, which could influence whole body metabolism, blood pressure, endothelial function and inflammatory responses [15,18,33,34], ultimately interfering with myocardial structure and function. Compared to global GPER KO mice [32], this study demonstrated that GPER deletion specifically in cardiomyocytes impaired heart structure and functions not only in male, but also in female mice.

The sex hormones, including the estrogens, play important roles in maintaining cardiac structure and function in both females and males [35]. Results from this study demonstrate that GPER expression levels in cardiomyocytes are the same in WT mice of both sexes; however, the effects of GPER deletion in cardiomyocytes on LV dimensions had different effects in males and females. Male mice with cardiomyocyte-specific GPER deletion exhibited profound increases in both LVEDD and LVESD compared to their female GPER KO mice. RWT was lower in male cardiomyocyte-specific GPER KO mice compared to WT male mice, whereas in female GPER KO mice, RWT was higher compared to WT mice. This interaction between sex and cardiomyocyte-specific GPER gene deletion accounted for nearly 19% of the total variance in RWT. Studies of global GPER KO mice also found that both systolic and diastolic function were impaired in males, but not females [32]. Consistent with the observed sex differences in cardiac structure and function with cardiomyocyte-specific GPER deletion, we found differential expression of cardiomyocyte genes in the male vs. female KO mice, providing a set of foundational data for future studies aimed at ascertaining the mechanisms underlying sex differences in cardioprotection by GPER.

The different effects of GPER deletion in LVESD, LVEDD, and the gene expression profiles between male and female mice might be due to the effects of endogenous estrogens in female mice through its other receptors, ERα and ERβ, which also play important roles in cardioprotection, in addition to GPER. In ovariectomized female rats, the ERβ agonist 8β-VE2 attenuates DOCA-induced hypertension and cardiac hypertrophy [36], while ERβ deletion augments the transverse aortic constriction (TAC)-induced cardiac hypertrophy in both male and female mice [37,38]. The functional roles of ERα in the heart are not consistent. While the activation of ERα by its agonist attenuates cardiac hypertrophy and improves heart function in TAC, spontaneous hypertensive, and DOCA animal models [36,39,40], ERα KO mice develop cardiac hypertrophy after TAC to the same extent as that in WT littermate [38]. More studies are needed to determine the exact roles of the individual estrogen receptors and their interactions in response to various stresses in the female versus the male heart.

A variety of pathways and mechanisms may mediate the cardioprotective effects of GPER. Using GSEA, we found that mitochondrial genes were enriched in GPER KO vs. WT cardiomyocytes from female, but not male, mice. Previous studies suggest that estrogens have significant regulatory roles in maintaining normal mitochondrial properties by stabilizing the structural assembly of mitochondria, attenuating mitochondrial ROS production, and modulating mitochondrial ATP synthesis in the heart [41]. The protective effects of estrogens might be mediated, at least partially, by GPER, since activation of GPER by G1 inhibits mitochondria permeability transition pore opening and protects the heart against ischemia-reperfusion injury [28]. More recently, studies in H9c2 cardiomyocytes

have shown that G1 mimics the beneficial actions of estradiol on enhancing mitochondrial function and biogenesis, while the GPER antagonist G15 neutralizes the beneficial effects on bioenergetics [42]. Although confirmation of any alterations in mitochondrial structure and function between cardiomyocyte-specific GPER KO vs. WT mice will require further study, our microarray data and GSEA provided direct evidence that the cardioprotective effects of GPER in the female might be related to enhancements in mitochondrial function.

In addition to the mitochondria gene changes, GSEA revealed that inflammatory response genes were enriched in GPER KO vs. WT cardiomyocytes, specifically among males. Previous studies suggest that the anti-inflammatory effects of estrogens might mediate cardioprotection [43–46]. Moreover, the agonist to GPER, G1, has been shown to inhibit inflammatory changes induced by tumor necrosis factor (TNF) in human umbilical vein endothelial cells [47,48]. However, the exact role of GPER on mediating the inflammatory responses of cardiomyocytes to various stressors remains unclear. The gene expression profile in GPER KO vs. WT cardiomyocytes suggest that GPER might mediate the anti-inflammatory actions of estrogens, and that the anti-inflammatory effects of GPER in cardiomyocytes is sex-specific.

5.0 Limitations and future studies

The present study focused on the gene expression profiles in cardiomyocytes of GPER KO mice which provides foundational information for further studies on the mechanisms underlying sex-specific cardioprotection by GPER. In order to get a high yield of adult cardiomyocytes with high quality, the cardiomyocyte isolation had to be performed immediately after the hearts were removed from the chest. Therefore, heart weights and morphology were not determined in this study. Future studies are in progress emphasizing potential GPER-related alterations in whole heart morphometric and histopathology, as well as single cardiomyocyte functional dynamics.

We also determined ERβ mRNA in cardiomyocytes using real-time PCR. We realize that some investigators report that ERβ is not detectable in the heart [49,50], while its existence in both cardiomyocytes and cardiac fibroblasts has been demonstrated at mRNA and protein levels, and might mediate the cardioprotective effects of estrogen [51–57]. Even though ERβ expression is not the focus of the present study, future investigations using a more specific ERβ antibody and/or PCR product sequencing are needed to confirm whether ERβ is expressed in the heart.

In summary, cardiomyocyte-specific GPER KO in mice induced adverse alterations in cardiac morphology and abnormalities in systolic and diastolic function, with different effects in males and females. Moreover, cardiomyocyte gene expression profile changes with the loss of GPER may also be influenced by sex, particularly for the families of genes relating to mitochondrial and inflammatory responses. Along with the powerful tool of the cardiomyocyte-specific GPER KO mouse model, the microarray data generated in this study provides the necessary foundation for ascertaining the exact roles of GPER in the heart and the underlying mechanisms of sex-specific cardioprotection in future studies.

Supplementary Material

Refer to Web version on PubMed Central for supplementary material.

Acknowledgments

The GPER mouse strain used for this research project was created from ES cell clone (EPD0334_2_H06) generated by the Wellcome Trust Sanger Institute and made into mice by the KOMP Repository (WWW.KOMP.org) and the Mouse Biology Program (www.mousebiology.org) at the University of California Davis. The mouse strain used for this research project, C57BL/6N-Tg(CAG-Flpo)1Afst/Mmucd, identification number 036512-UCD, was obtained from the Mutant Mouse Regional Resource Center (MMRRC) at UC Davis, a NIH funded strain repository, and was originally donated to the MMRRC by Dr. Konstantinos Anastassiadis from Technische Universitaet Dresden. We appreciate the assistance of Ms. Lou Craddock at Wake Forest University Comprehensive Cancer Center Microarray facility in running the microarray. This work was funded by National Institutes of Health Grants AG-042758 (L.G.), AG-033727 (L.G.), and HL-051952 (C.M.F.).

References

1. Mozaffarian D, Benjamin EJ, Go AS, Arnett DK, Blaha MJ, Cushman M, et al. Heart disease and stroke statistics--2015 update: a report from the American Heart Association. Circulation. 2015; 131:e29–e322. [PubMed: 25520374]
2. Mosca L, Benjamin EJ, Berra K, Bezanson JL, Dolor RJ, Lloyd-Jones DM, et al. Effectiveness-based guidelines for the prevention of cardiovascular disease in women--2011 update: a guideline from the American Heart Association. J. Am. Coll. Cardiol. 2011; 57:1404–1423. [PubMed: 21388771]
3. Kelsey SF, James M, Holubkov AL, Holubkov R, Cowley MJ, Detre KM. Results of percutaneous transluminal coronary angioplasty in women. 1985–1986 National Heart, Lung, and Blood Institute's Coronary Angioplasty Registry. Circulation. 1993; 87:720–727. [PubMed: 8443892]
4. Lloyd-Jones D, Adams RJ, Brown TM, Carnethon M, Dai S, De Simone G, et al. Heart disease and stroke statistics--2010 update: a report from the American Heart Association. Circulation. 2012; 121:e46–e215.
5. Boardman H, Hartley L, Eisinga A, Main C, Figuls MR. Cochrane corner: oral hormone therapy and cardiovascular outcomes in post-menopausal women. Heart. 2016; 102:9–11. [PubMed: 26453279]
6. Hale GE, Shufelt CL. Hormone therapy in menopause: An update on cardiovascular disease considerations. Trends. Cardiovasc. Med. 2015; 25:540–549. [PubMed: 26270318]
7. Hvidtfeldt UA, Tjønneland A, Keiding N, Lange T, Andersen I, Sørensen TI, et al. Risk of breast cancer in relation to combined effects of hormone therapy, body mass index, and alcohol use, by hormone-receptor status. Epidemiology. 2015; 26:353–361. [PubMed: 25695354]
8. Bassuk SSJE. The timing hypothesis: Do coronary risks of menopausal hormone therapy vary by age or time since menopause onset? Metabolism. 2016; 65:794–803. [PubMed: 27085786]
9. Owman C, Blay P, Nilsson C, Lolait SJ. Cloning of human cDNA encoding a novel heptahelix receptor expressed in Burkitt's lymphoma and widely distributed in brain and peripheral tissues. Biochem. Biophys. Res. Commun. 1996; 228:285–292. [PubMed: 8920907]
10. Deschamps AM, Murphy E. Activation of a novel estrogen receptor, GPER, is cardioprotective in male and female rats. Am. J. Physiol. Heart. Circ. Physiol. 2009; 297:H1806–H1813. [PubMed: 19717735]
11. Wang H, Jessup JA, Lin MS, Chagas C, Lindsey SH, Groban L. Activation of GPR30 attenuates diastolic dysfunction and left ventricle remodelling in oophorectomized mRen2. Lewis rats. Cardiovasc. Res. 2012; 94:96–104. [PubMed: 22328091]
12. Zhao Z, Wang H, Jessup JA, Lindsey SH, Chappell MC, Groban L. Role of estrogen in diastolic dysfunction. Am. J. Physiol. Heart. Circ. Physiol. 2004; 306:H628–H640.
13. Alencar AK, da Silva JS, Lin M, Silva AM, Sun X, Ferrario CM, et al. Effect of age, estrogen status, and late-Life GPER activation on cardiac structure and function in the Fischer344×Brown Norway female rat. J. Gerontol. A. Biol. Sci. Med. Sci. 2016 Mar 22. pii: glw045. [Epub ahead of print].

14. Wang C, Lv X, Jiang CJS. The putative G-protein coupled estrogen receptor agonist G-1 suppresses proliferation of ovarian and breast cancer cells in a GPER-independent manner. Am. J. Transl. Res. 2012; 4:390–402. [PubMed: 23145207]
15. Sharma G, Prossnitz ER. GPER/GPR30 Knockout Mice: Effects of GPER on metabolism. Methods. Mol. Biol. 2016; 1366:489–502. [PubMed: 26585159]
16. Meoli L, Isensee J, Zazzu V, Nabzdyk CS, Soewarto D, Witt H, et al. Sex- and age-dependent effects of Gpr30 genetic deletion on the metabolic and cardiovascular profiles of diet-induced obese mice. Gene. 2014; 540:210–216. [PubMed: 24582972]
17. Ford J, Hajibeigi A, Long M, Hahner L, Gore C, Hsieh JT, et al. GPR30 deficiency causes increased bone mass, mineralization, and growth plate proliferative activity in male mice. J. Bone. Miner. Res. 2011; 26:298–307. [PubMed: 20734455]
18. Li Z, Cheng L, Liang H, Duan W, Hu J, Zhi W, et al. GPER inhibits diabetes-mediated RhoA activation to prevent vascular endothelial dysfunction. Eur. J. Cell. Biol. 2016; 95:100–113. [PubMed: 26785611]
19. Gui Y, Shi Z, Wang Z, Li JJ, Xu C, Tian R, et al. The GPER agonist G-1 induces mitotic arrest and apoptosis in human vascular smooth muscle cells independent of GPER. J. Cell. Physiol. 2015; 230:885–895. [PubMed: 25204801]
20. Wang H, Zhao Z, Lin M, Groban L. Activation of GPR30 inhibits cardiac fibroblast proliferation. Mol. Cell. Biochem. 2015; 405:135–148. [PubMed: 25893735]
21. Zhao Z, Wang H, Lin M, Groban L. GPR30 decreases cardiac chymase/angiotensin II by inhibiting local mast cell number. Biochem. Biophys. Res. Commun. 2015; 459:131–136. [PubMed: 25712524]
22. Skarnes WC, Rosen B, West AP, Koutsourakis M, Bushell W, Iyer V, et al. A conditional knockout resource for the genome-wide study of mouse gene function. Nature. 2011; 474:337–342. [PubMed: 21677750]
23. Bharadwaj MS, Strawn WB, Groban L, Yamaleyeva LM, Chappell MC, Horta C, et al. Angiotensin-converting enzyme 2 deficiency is associated with impaired gestational weight gain and fetal growth restriction. Hypertension. 2011; 58:852–858. [PubMed: 21968754]
24. Bolstad BM, Irizarry RA, Astrand M, Speed TP. A comparison of normalization methods for high density oligonucleotide array data based on variance and bias. Bioinformatics. 2003; 19:185–193. [PubMed: 12538238]
25. Smyth GK. Linear models and empirical Bayes methods for assessing differential expression in microarray experiments. Stat. Appl. Genet. Mol. Biol. 2004; 3 Article3.
26. Chou JW, Zhou T, Kaufmann WK, Paules RS, Bushel PR. Extracting gene expression patterns and identifying co-expressed genes from microarray data reveals biologically responsive processes. BMC. Bioinformatics. 2007; 8:427. [PubMed: 17980031]
27. Wang H, Sun X, Chou J, Lin M, Ferrario CM, Zapata-Sudo G, Groban L. Inflammatory and mitochondrial gene expression data in GPER-deficient cardiomyocytes from male and female mice. Data In Brief (Submitted for publication).
28. Bopassa JC, Eghbali M, Toro L, Stefani E. A novel estrogen receptor GPER inhibits mitochondria permeability transition pore opening and protects the heart against ischemia-reperfusion injury. Am. J. Physiol. Heart. Circ. Physiol. 2010; 298:H16–H23. [PubMed: 19880667]
29. Filice E, Recchia AG, Pellegrino D, Angelone T, Maggiolini M, Cerra MC. A new membrane G protein-coupled receptor (GPR30) is involved in the cardiac effects of 17beta-estradiol in the male rat. J. Physiol. Pharmacol. 2009; 60:3–10.
30. Weil BR, Manukyan MC, Herrmann JL, Wang Y, Abarbanell AM, Poynter JA, et al. Signaling via GPR30 protects the myocardium from ischemia/reperfusion injury. Surgery. 2010; 148:436–443. [PubMed: 20434187]
31. Jessup JA, Lindsey SH, Wang H, Chappell MC, Groban L. Attenuation of salt-induced cardiac remodeling and diastolic dysfunction by the GPER agonist G-1 in female mRen2.Lewis rats. PLoS. One. 2010; 5:e15433. [PubMed: 21082029]
32. Delbeck M, Golz S, Vonk R, Janssen W, Hucho T, Isensee J, et al. Impaired left-ventricular cardiac function in male GPR30-deficient mice. Mol. Med. Rep. 2011; 4:37–40. [PubMed: 21461560]

33. Zimmerman MA, Budish RA, Kashyap S, Lindsey SH. GPER-novel membrane estrogen receptor. Clin. Sci. (Lond). 2016; 130:1005–1016. [PubMed: 27154744]
34. Zhao TZ, Ding Q, Hu J, He SM, Shi F, Ma LT. GPER expressed on microglia mediates the anti-inflammatory effect of estradiol in ischemic stroke. Brain. Behav. 2016; 6:e00449. [PubMed: 27127723]
35. De Smet MA, Lapauw B, De Backer T. Sex steroids in relation to cardiac structure and function in men. Andrologia. 2016 May 2. [Epub ahead of print].
36. Arias-Loza PA, Hu K, Dienesch C, Mehlich AM, König S, Jazbutyte V, et al. Both estrogen receptor subtypes, alpha and beta, attenuate cardiovascular remodeling in aldosterone salt-treated rats. Hypertension. 2007; 50:432–438. [PubMed: 17562975]
37. Fliegner D, Schubert C, Penkalla A, Witt H, Kararigas G, Dworatzek E, et al. Female sex and estrogen receptor-beta attenuate cardiac remodeling and apoptosis in pressure overload. Am. J. Physiol. Regul. Integr. Comp. Physiol. 2010; 298 R1597-F1606.
38. Skavdahl M, Steenbergen C, Clark J, Myers P, Demianenko T, Mao L, et al. Estrogen receptor-beta mediates male-female differences in the development of pressure overload hypertrophy. Am. J. Physiol. Heart. Circ. Physiol. 2005; 288:H469–H476. [PubMed: 15374829]
39. Pelzer T, Jazbutyte V, Hu K, Segerer S, Nahrendorf M, Nordbeck P, et al. The estrogen receptor-alpha agonist 16alpha-LE2 inhibits cardiac hypertrophy and improves hemodynamic function in estrogen-deficient spontaneously hypertensive rats. Cardiovasc. Res. 2005; 67:604–612. [PubMed: 15950203]
40. Westphal C, Schubert C, Prelle K, Penkalla A, Fliegner D, Petrov G, et al. Effects of estrogen, an ERα agonist and raloxifene on pressure overload induced cardiac hypertrophy. PLoS. One. 2012; 7:e50802. [PubMed: 23227210]
41. Rattanasopa C, Phungphong S, Wattanapermpool J, Bupha-Intr T. Significant role of estrogen in maintaining cardiac mitochondrial functions. J. Steroid. Biochem. Mol. Biol. 2015; 147:1–9. [PubMed: 25448746]
42. Sbert-Roig M, Bauzá-Thorbrügge M, Galmés-Pascual BM, Capllonch-Amer G, García-Palmer FJ, Lladó I, et al. GPER mediates the effects of 17β-estradiol in cardiac mitochondrial biogenesis and function. Mol. Cell. Endocrinol. 2016; 420:116–124. [PubMed: 26628039]
43. McLarty JL, Li J, Levick SP, Janicki JS. Estrogen modulates the influence of cardiac inflammatory cells on function of cardiac fibroblasts. J. Inflamm. Res. 2013; 6:99–108. [PubMed: 24062614]
44. Zhu X, Tang Z, Cong B, Du J, Wang C, Wang L, et al. Estrogens increase cystathionine-γ-lyase expression and decrease inflammation and oxidative stress in the myocardium of ovariectomized rats. Menopause. 2013; 20:1084–1091. [PubMed: 23571523]
45. Pechenino AS, Lin L, Mbai FN, Lee AR, He XM, Stallone JN, et al. Impact of aging vs. estrogen loss on cardiac gene expression: estrogen replacement and inflammation. Physiol. Genomics. 2011; 43:1065–1073. [PubMed: 21750230]
46. Stice JP, Chen L, Kim SC, Jung JS, Tran AL, Liu TT, et al. 17β-Estradiol, aging, inflammation, and the stress response in the female heart. Endocrinology. 2011; 152:1589–1598. [PubMed: 21303943]
47. Chakrabarti S, Davidge ST. Analysis of G-protein coupled receptor 30 (GPR30) on endothelial inflammation. Methods. Mol. Biol. 2016; 1366:503–516. [PubMed: 26585160]
48. Chakrabarti S, Davidge ST. G-protein coupled receptor 30 (GPR30): a novel regulator of endothelial inflammation. PLoS. One. 2012; 7:e52357. [PubMed: 23285008]
49. Pugach EK, Blenck CL, Dragavon JM, Langer SJ, Leinwand LALA. Estrogen receptor profiling and activity in cardiac myocytes. Mol. Cell. Endocrinol. 2016; 431:62–70. [PubMed: 27164442]
50. Förster C, Kietz S, Hultenby K, Warner M, Gustafsson JA. Characterization of the ERbeta−/−mouse heart. Proc. Natl. Acad. Sci. U. S. A. 2004; 101:14234–14239. [PubMed: 15375213]
51. Irsik DL, Carmines PK, Lane PH. Classical estrogen receptors and ERα splice variants in the mouse. PLoS. One. 2013; 8:e70926. [PubMed: 23940668]
52. Schuster I, Mahmoodzadeh S, Dworatzek E, Jaisser F, Messaoudi S, Morano I, Regitz-Zagrosek V. Cardiomyocyte-specific overexpression of oestrogen receptor β improves survival and cardiac function after myocardial infarction in female and male mice. Clin. Sci. (Lond). 2016; 130:365–376. [PubMed: 26608078]

53. Gao J, Xu D, Sabat G, Valdivia H, Xu W, Shi NQ. Disrupting KATP channels diminishes the estrogen-mediated protection in female mutant mice during ischemia-reperfusion. Clin. Proteomics. 2014; 11:19. [PubMed: 24936167]

54. Pfaffl MW, Lange IG, Daxenberger A, Meyer HH. Tissue-specific expression pattern of estrogen receptors (ER): quantification of ER alpha and ER beta mRNA with real-time RT-PCR. APMIS. 2001; 109:345–355. [PubMed: 11478682]

55. Watanabe T, Akishita M, He H, Miyahara Y, Nagano K, Nakaoka T, et al. 17 beta-estradiol inhibits cardiac fibroblast growth through both subtypes of estrogen receptor. Biochem. Biophys. Res. Commun. 2003; 311:454–459. [PubMed: 14592435]

56. Saunders PT, Fisher JS, Sharpe RM, Millar MR. Expression of oestrogen receptor beta (ER beta) occurs in multiple cell types, including some germ cells, in the rat testis. J. Endocrinol. 1998; 156:R13–R17. [PubMed: 9582517]

57. Grohé C, Kahlert S, Löbbert K, Stimpel M, Karas RH, Vetter H, et al. Cardiac myocytes and fibroblasts contain functional estrogen receptors. FEBS. Lett. 1997; 416:107–112. [PubMed: 9369244]

Highlights

- Cardiomyocyte-specific GPER knockout leads to left ventricular dysfunction.
- Effects of GPER knockout in the heart are sex-dependent.
- GPER in the female heart is related to the enhancements in mitochondrial function.
- Inflammatory response genes are enriched in male GPER knockout cardiomyocytes.

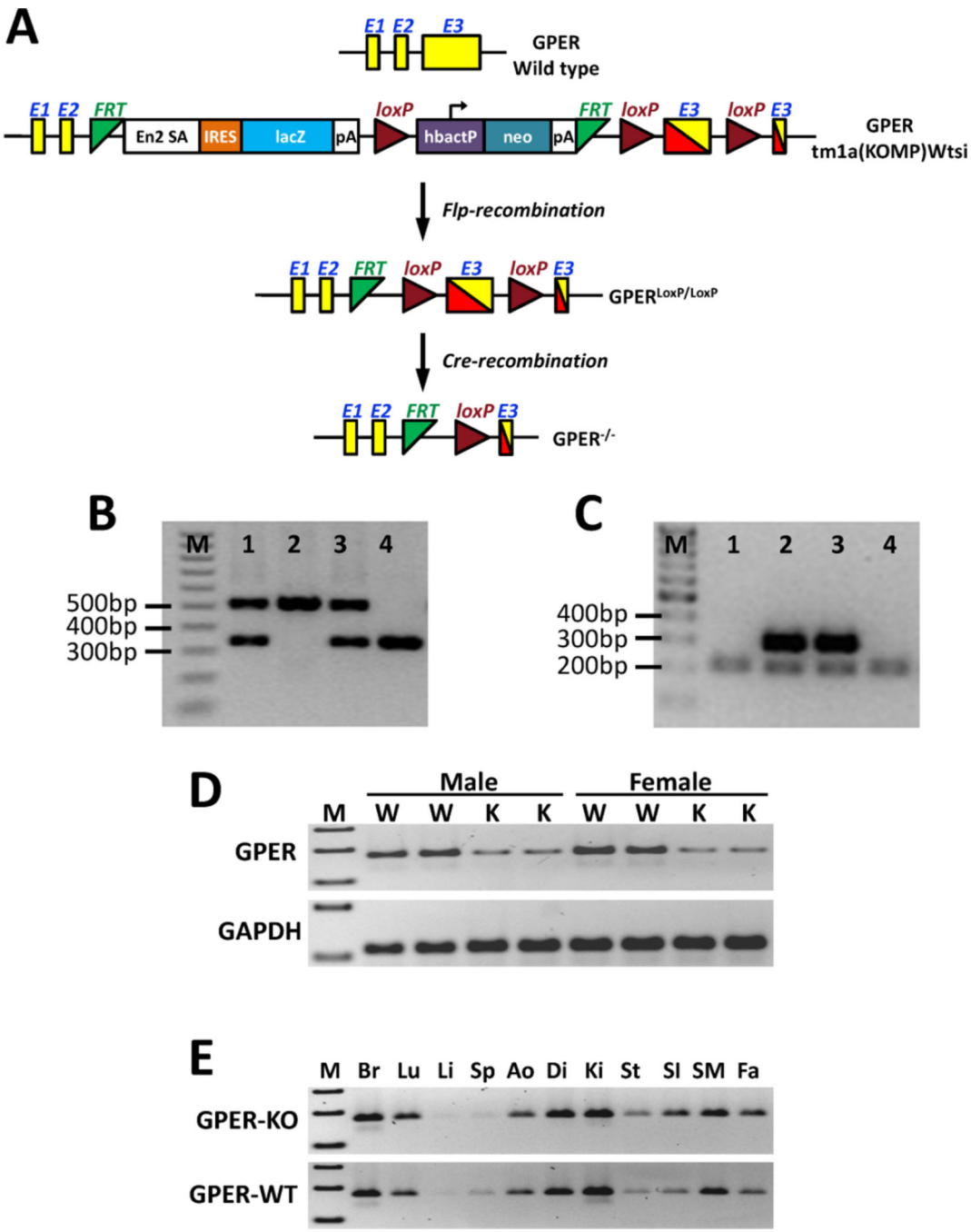

Figure 1.

Development of the cardiomyocyte-specific GPER KO mouse. (A) Targeting strategy for the conditional disruption of the GPER gene. (B) A representative image showing genotyping results for the floxed GPER transgene from mouse tails. Sample 2: 530 bp band, homozygous floxed GPER transgene ($GPER^{f/f}$); Sample 4: 345 bp band, WT GPER; Samples 1 and 3: 530 bp and 345 bp bands, heterozygous floxed GPER transgene. (C) A representative image showing genotyping results for the Cre transgenic mice. Samples 2 and 3: 300 bp band, Cre positive; Samples 1 and 4: 200 bp band, Cre negative (internal positive

control for PCR). (D) RT-PCR results showing knockdown of GPER expression in cardiomyocytes isolated from adult (8 weeks old) $GPER^{f/f/Cre}$ mice (knockout, K) compared with $GPER^{f/f}$ mice (W). (E) RT-PCR results showing GPER expression in various tissues from $GPER^{f/f/Cre}$ (knockout, KO) vs. $GPER^{f/f}$ (WT) mice. M: marker; Br: brain; Lu: lung; Li: liver; Sp: spleen; Ao: aorta; Di: diaphragm; Ki: kidney; St: stomach; SI: small intestine; SM: skeletal muscle; Fa: fat.

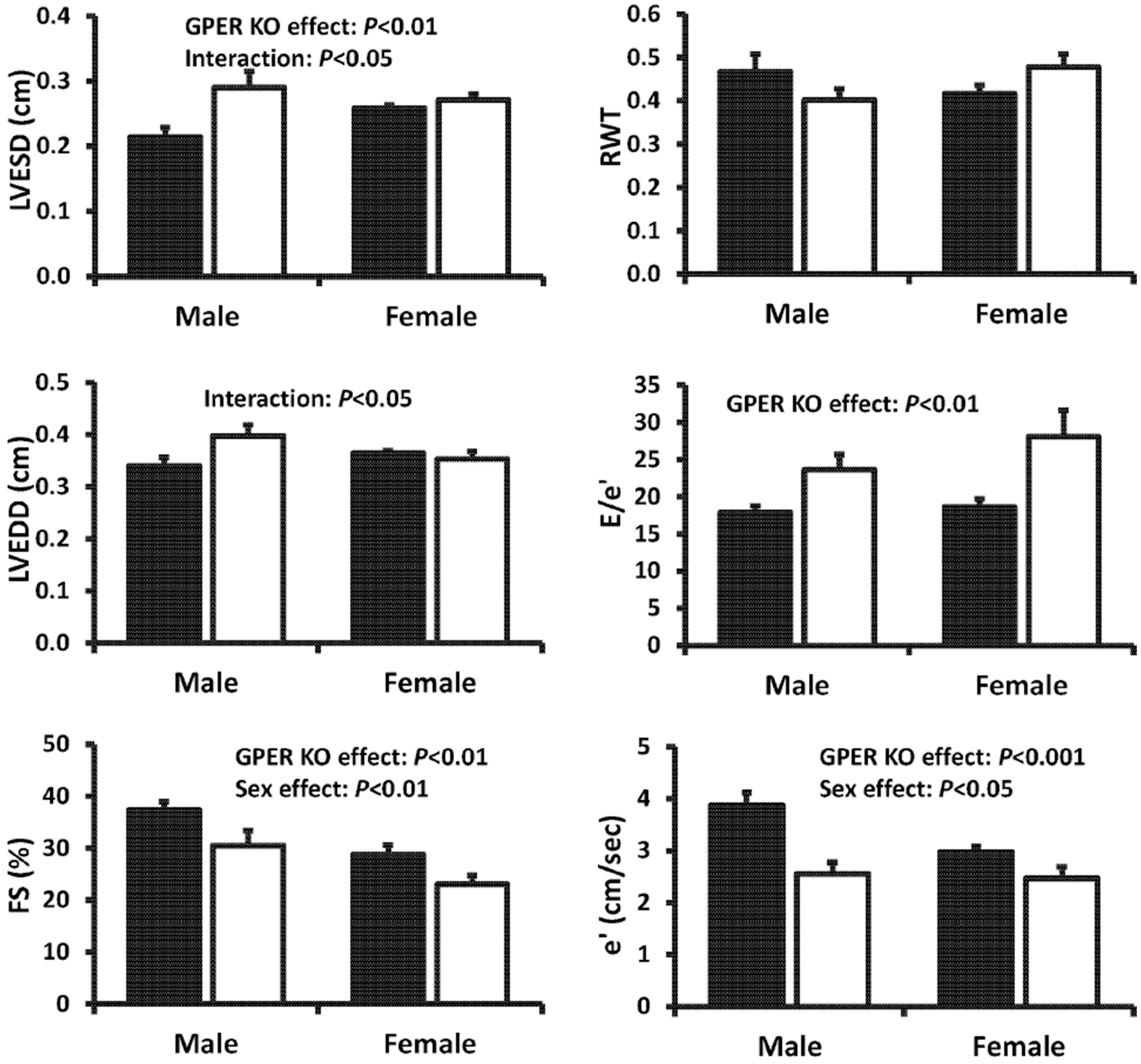

Figure 2.

Echocardiographic measurements in cardiomyocyte-specific GPER KO (open bar) vs. WT (GPER intact, solid bar) mice. Values are means ± SEM; n=4/group. Two-way ANOVA was used to determine the significant differences with respect to sex (male vs. female), GPER status (WT vs. KO), and the interaction (sex × GPER status).

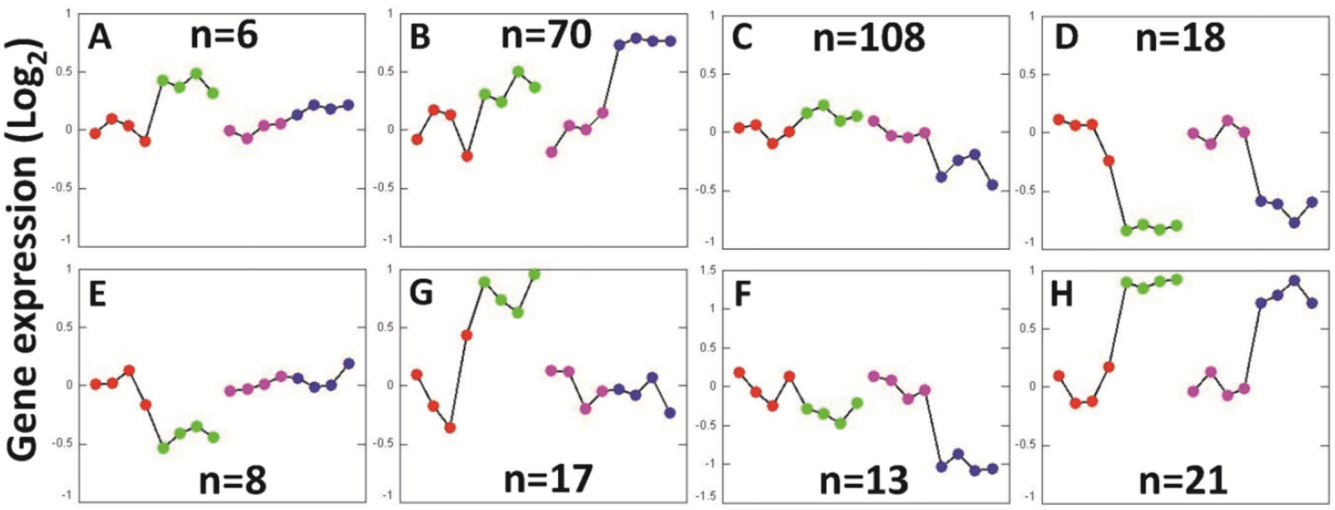

Figure 3.

Gene expression patterns extracted by EPIG from microarray data from cardiomyocyte-specific GPER KO and WT (GPER intact) mice. The *y*-axis is the average $\log_2$ of the ratio values from the top 6 gene probe set profiles within the respective pattern. The average expression levels in one of the WT female mice were aligned around 0 (*y*-axis) in the EPIG analysis. Each point along the *x*-axis represents a mouse sample. Within a single pattern from left to right: WT female (red), GPER KO female (green), WT male (pink), and GPER KO male (blue). The numbers of significant genes for each pattern are shown in the figures.

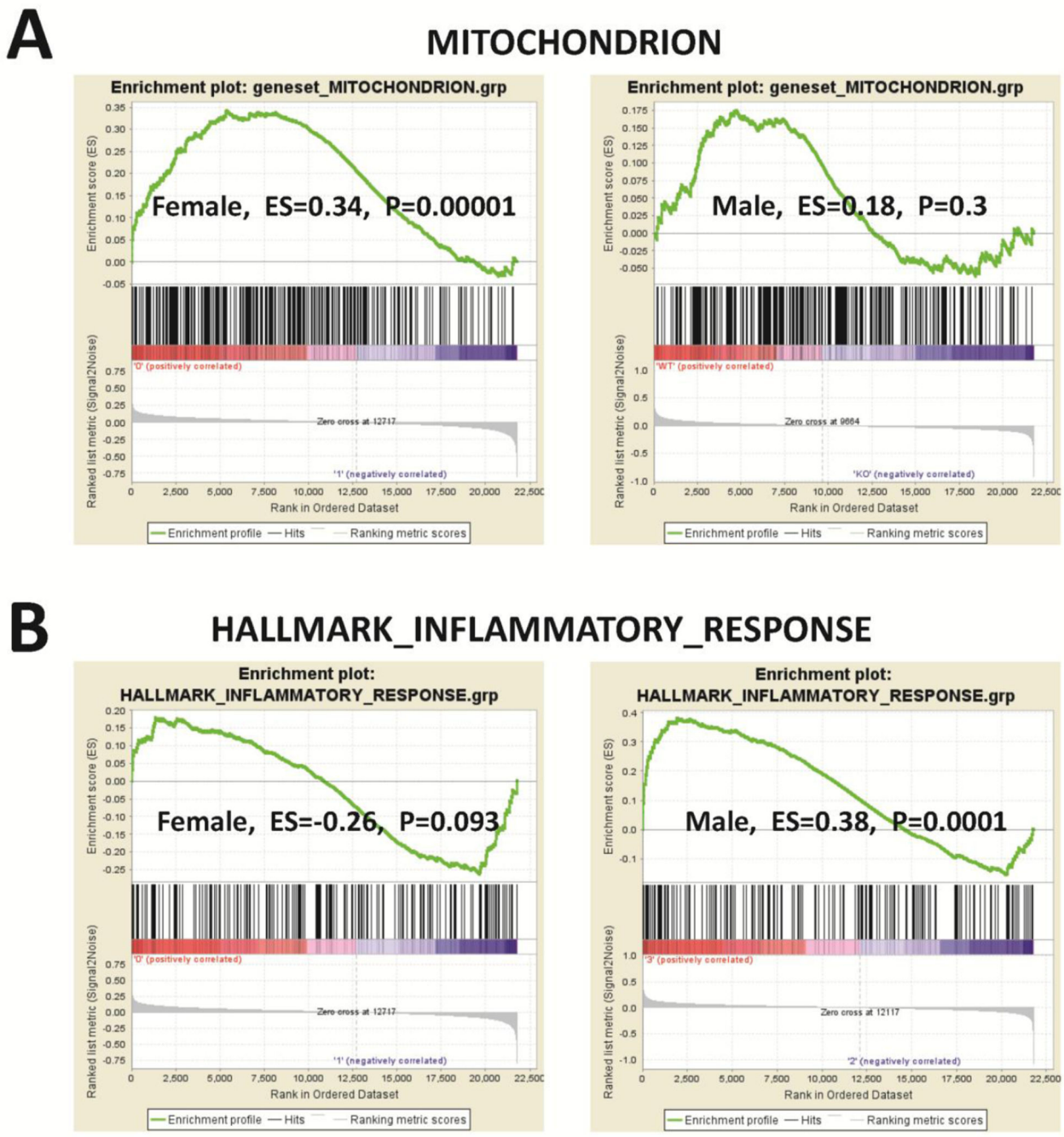

Figure 4.

GSEA analysis for the enrichment of “MITOCHONDRION (including 314 genes)” and “HALLMARK_INFLAMMATORY_RESPONSE (including 193 genes)” gene sets in cardiomyocyte-specific GPER KO vs. WT (GPER intact) cardiomyocytes. The bar-code plot indicates the positions of genes in each gene set; red and blue colors represent positive and negative Pearson correlations with GPER expression, respectively. The results show that mitochondrial genes were enriched in GPER KO vs. WT cardiomyocytes from female, but

not male, mice. Inflammatory response genes were enriched in GPER KO vs. WT cardiomyocytes from male, but not female, mice. ES: enrichment score.

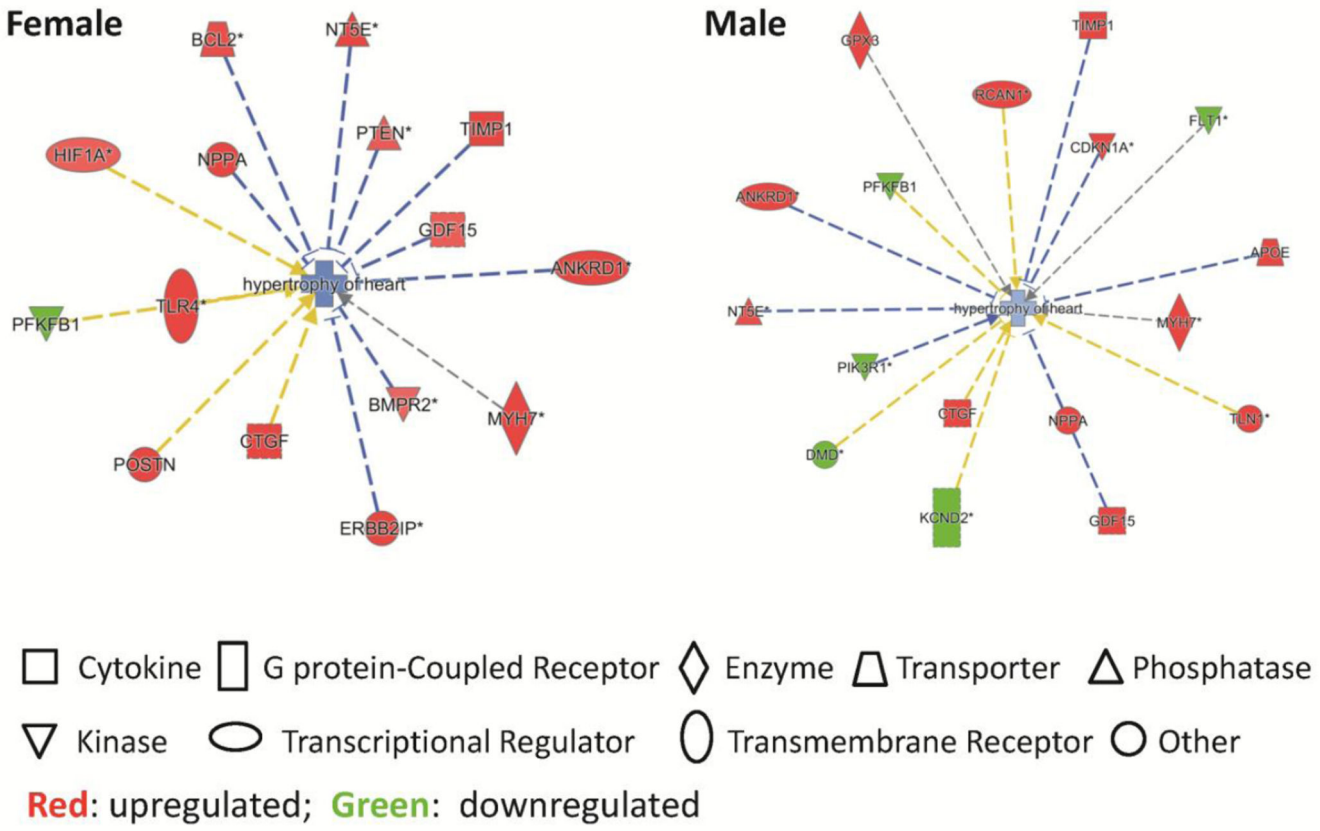

Figure 5.
Cardiac hypertrophy-related gene expression analyzed by the IPA software.

Table 1

Body weight, systolic BP, treadmill time, selected gene mRNA levels in cardiomyocytes

	Male		Female		*P* Values		
	WT	**KO**	**WT**	**KO**	**Sex**	**KO**	**Sex×KO**
n	4	4	4	4			
Body weight (g)	31.1 ± 0.8	28.0 ± 0.5	22.4 ± 0.9	22.4 ± 0.8	<0.0001	0.068	0.059
Systolic BP (mmHg)	108 ± 4	114 ± 3	109 ± 2	111 ± 2	0.813	0.223	0.544
Treadmill time (min)	18.8 ± 1.6	21.5 ± 1.6	33.6 ± 2.6	28.9 ± 1.9	<0.0001	0.624	0.117
Gene mRNA levels in cardiomyocytes							
GPER	1.00 ± 0.08	0.44 ± 0.04	1.16 ± 0.26	0.39 ± 0.04	0.394	<0.001	0.081
ERα	1.00 ± 0.15	0.81 ± 0.07	0.87 ± 0.07	0.99 ± 0.24	0.869	0.814	0.320
ERβ	1.00 ± 0.14	0.81 ± 0.04	0.85 ± 0.12	0.79 ± 0.14	0.301	0.472	0.625
ANF	1.00 ± 0.27	3.38 ± 0.16	1.07 ± 0.18	3.73 ± 0.28	0.371	<0.0001	0.555
BNP	1.00 ± 0.11	2.25 ± 0.45	1.59 ± 0.33	2.97 ± 0.72	0.179	0.014	0.880

WT: wild type ($GPER^{f/f}$); KO: cardiomyocyte-specific GPER knockout ($GPER^{f/f/Cre}$); BP: blood pressure; ER: estrogen receptor; ANF: atrial natriuretic factor; BNP: brain natriuretic peptide. Two-way ANOVA was used to determine the significant differences in respect to sex (male vs. female), GPER status (WT vs. KO), and interaction (gender × GPER status).

Table 2

Top 50 most significantly upregulated genes in cardiomyocytes of female cardiomyocyte-specific GPER KO vs. WT mice

Gene Symbol	Gene Description	Fold Change	*P* Value
Myh7	myosin, heavy polypeptide 7, cardiac muscle, beta	6.87	0.00000
2810474O19Rik	RIKEN cDNA 2810474O19 gene	3.32	0.00130
Tmem 184c	transmembrane protein 184C	2.73	0.00011
Ndnf	neuron-derived neurotrophic factor	2.72	0.00000
Fgl2	fibrinogen-like protein 2	2.63	0.00003
Xist	inactive X specific transcripts	2.62	0.00028
Malat1	metastasis associated lung adenocarcinoma transcript 1	2.46	0.01767
Trpm7	transient receptor potential cation channel, member M7	2.35	0.01411
Acta1	actin, alpha 1, skeletal muscle	2.28	0.00318
Nppa	natriuretic peptide type A	2.26	0.00014
Ankrd1	ankyrin repeat domain 1 (cardiac muscle)	2.22	0.00000
Gck	glucokinase	2.21	0.00001
Phldb2	pleckstrin homology-like domain, family B, member 2	2.17	0.00014
Mybpc2	myosin binding protein C, fast-type	2.14	0.00000
Zfp445	zinc finger protein 445	2.11	0.00874
Kdm7a	lysine (K)-specific demethylase 7A	2.09	0.00391
Dmxl2	Dmx-like 2	2.06	0.00088
Fam 198b	family with sequence similarity 198, member B	2.06	0.00062
Sorbs2	sorbin and SH3 domain containing 2	2.05	0.01998
Atrx	α thalassemia/mental retardation syndrome X-linked homolog	2.04	0.02410
Nbeal1	neurobeachin like 1	2.04	0.01435
Kif5b	kinesin family member 5B	2.02	0.00769
Gas5/Snord47	growth arrest specific 5/small nucleolar RNA, C/D box 47	1.98	0.03187
Rtn4	reticulon 4	1.98	0.00000
Rif1	Rap 1 interacting factor 1 homolog (yeast)	1.94	0.01003
Akap9	A kinase (PRKA) anchor protein (yotiao) 9	1.92	0.02423
Tlr4	toll-like receptor 4	1.92	0.00132
Arid4b	AT rich interactive domain 4B (RBPl-like)	1.91	0.00883
Trove2	TROVE domain family, member 2	1.90	0.00000
Gdap10	ganglioside-induced differentiation-associated-protein 10	1.90	0.02673
Cfh	complement component factor h	1.90	0.01042
Ranbp2	RAN binding protein 2	1.89	0.01033
Kif5b	kinesin family member 5B	1.87	0.01335
Trip 11	thyroid hormone receptor interactor 11	1.85	0.00204
Cwf1912	CWF19-like 2, cell cycle control (*S. pombe*)	1.85	0.01437
Acbd5	acyl-Coenzyme A binding domain containing 5	1.84	0.02449
H2-Aa	histocompatibility 2, class II antigen A, alpha	1.84	0.00074

Gene Symbol	Gene Description	Fold Change	*P* Value
Usp9x	ubiquitin specific peptidase 9, X chromosome	1.81	0.00489
Zfp367	zinc finger protein 367	1.81	0.00794
Ccnd2	cyclin D2	1.80	0.00014
Lin7c	lin-7 homolog C (*C. elegans*)	1.80	0.04039
Pcolce	procollagen C-endopeptidase enhancer protein	1.79	0.00052
Zfp62	zinc finger protein 62	1.79	0.03314
Phlda3	pleckstrin homology-like domain, family A, member 3	1.79	0.00000
Pnisr	PNN interacting serine/arginine-rich	1.79	0.04485
Lgals3	lectin, galactose binding, soluble 3	1.79	0.00888
Pde1c	phosphodiesterase 1C	1.78	0.00067
Cast	calpastatin	1.78	0.01134
Nabp1	nucleic acid binding protein 1	1.78	0.00223
Taok1	TAO kinase 1	1.77	0.01954

Table 3

Top 50 most significantly upregulated genes in cardiomyocytes of male cardiomyocyte-specific GPER KO vs. WT mice

Gene Symbol	Gene Description	Fold Change	*P* Value
Myh7	myosin, heavy polypeptide 7, cardiac muscle, beta	7.26	0.00000
Ndnf	neuron-derived neurotrophic factor	3.48	0.00000
Lgals3	lectin, galactose binding, soluble 3	3.15	0.00002
Timp1	tissue inhibitor of metalloproteinase 1	2.83	0.00000
Fgl2	fibrinogen-like protein 2	2.80	0.00001
H2-Aa	histocompatibility 2, class II antigen A, alpha	2.72	0.00000
Nppa	natriuretic peptide type A	2.65	0.00002
Ctss	cathepsin S	2.47	0.00016
Col3a1	collagen, type III, alpha 1	2.26	0.00555
Cdkn1a	cyclin-dependent kinase inhibitor 1A (P21)	2.23	0.00261
Phlda3	pleckstrin homology-like domain, family A, member 3	2.17	0.00000
Lyz1	lysozyme 1	2.17	0.00017
H2-Eb1	histocompatibility 2, class II antigen E beta	2.16	0.00013
Mybpc2	myosin binding protein C, fast-type	2.15	0.00000
Lcn2	lipocalin 2	2.12	0.00002
Lyz2	lysozyme 2	2.08	0.00023
Cd74	CD74 antigen	2.07	0.00000
Fcgr2b	Fc receptor, IgG, low affinity IIb	2.05	0.00044
Slc38a4	solute carrier family 38, member 4	2.04	0.00189
Tubb2a	tubulin, beta 2A class IIA	2.03	0.00025
Ccl 6	chemokine (C-C motif) ligand 6	2.01	0.00224
Nppb	natriuretic peptide type B	2.00	0.00017
Rtn4	reticulon 4	1.99	0.00000
Fam 198b	family with sequence similarity 198, member B	1.99	0.00095
Dpysl3	dihydropyrimidinase-like 3	1.98	0.00000
Pcolce	procollagen C-endopeptidase enhancer protein	1.93	0.00017
Tmem 176a	transmembrane protein 176A	1.91	0.00001
Hn 1	hematological and neurological expressed sequence 1	1.88	0.00000
Comtd 1	catechol-O-methyltransferase domain containing 1	1.86	0.00000
Socs3	suppressor of cytokine signaling 3	1.83	0.02286
Ctgf	connective tissue growth factor	1.83	0.00093
Tmem 176b	transmembrane protein 176B	1.83	0.00000
Ephx1	epoxide hydrolase 1, microsomal	1.81	0.00363
Mthfd2	methylenetetrahydrofolate dehydrogenase (NAD+ dependent), methenyltetrahydrofolate cyclohydrolase	1.80	0.00097
Stbd1	starch binding domain 1	1.80	0.00000
Ccl9	chemokine (C-C motif) ligand 9	1.80	0.00011
Ctsz	cathepsin Z	1.79	0.00021

Gene Symbol	Gene Description	Fold Change	*P* Value
Tyrobp	TYRO protein tyrosine kinase binding protein	1.78	0.00025
Apoe	apolipoprotein E	1.77	0.00090
Mt2	metallothionein 2	1.77	0.00207
C1qc	complement component 1, q subcomponent, C chain	1.77	0.00104
Acta1	actin, alpha 1, skeletal muscle	1.76	0.02983
H2-Aa	histocompatibility 2, class II antigen A, alpha	1.75	0.00240
Slc38a1	solute carrier family 38, member 1	1.75	0.00097
2610002J02Rik	RIKEN cDNA 2610002J02 gene	1.75	0.00069
H2-Ab1	histocompatibility 2, class II antigen A, beta 1	1.73	0.00001
Cpxm2	carboxypeptidase X 2 (M14 family)	1.71	0.04565
Tspo	translocator protein	1.70	0.00000
Scd2	stearoyl-Coenzyme A desaturase 2	1.70	0.00147
Grk5	G protein-coupled receptor kinase 5	1.70	0.00183

Table 4

Top 50 most significantly downregulated genes in cardiomyocytes of cardiomyocyte-specific GPER female KO vs. WT mice

Gene Symbol	Gene Description	Fold Change	*P* Value
Amy1	amylase 1, salivary	0.37	0.00002
Acot1	acyl-CoA thioesterase 1	0.41	0.00031
Il15	interleukin 15	0.50	0.00523
Ssbp2	single-stranded DNA binding protein 2	0.51	0.00000
Ano 10	anoctamin 10	0.52	0.00000
Dcakd	dephospho-CoA kinase domain containing	0.53	0.00000
Pfkfb1	6-phosphofructo-2-kinase/fructose-2,6-biphosphatase 1	0.53	0.00010
2310040G07Rik	RIKEN cDNA 2310040G07 gene	0.54	0.00915
1700040L02Rik	RIKEN cDNA 1700040L02 gene	0.54	0.00006
Exoc2	exocyst complex component 2	0.55	0.00000
Dmd	dystrophin, muscular dystrophy	0.56	0.07599
Maob	monoamine oxidase B	0.56	0.00000
Ucp3	uncoupling protein 3 (mitochondrial, proton carrier)	0.56	0.00810
Ctnna3	catenin (cadherin associated protein), alpha 3	0.56	0.00001
Aldob	aldolase B, fructose-bisphosphate	0.57	0.00022
Wif1	Wnt inhibitory factor 1	0.58	0.01025
Egflam	EGF-like, fibronectin type III and laminin G domains	0.58	0.00031
Acot2	acyl-CoA thioesterase 2	0.60	0.00067
G0s2	G0/G1 switch gene 2	0.60	0.00614
Acot1/Acot2	acyl-CoA thioesterase 1 / acyl-CoA thioesterase 2	0.60	0.00105
Immp2l	IMP2 inner mitochondrial membrane peptidase-like	0.60	0.00002
Sox4	SRY (sex determining region Y)-box 4	0.61	0.02574
Fdft1	farnesyl diphosphate farnesyl transferase 1	0.61	0.00068
Btg1	B cell translocation gene 1, anti-proliferative	0.61	0.00854
Csrp2	cysteine and glycine-rich protein 2	0.61	0.01669
Kcnj3	potassium inwardly-rectifying channel, subfamily J, member 3	0.61	0.00813
Fbp2	fructose bisphosphatase 2	0.64	0.00494
Tm4sf1	transmembrane 4 superfamily member 1	0.64	0.02878
Apbb1	amyloid beta precursor protein-binding, family B, member 1	0.65	0.00003
Tesc	tescalcin	0.65	0.00412
Ttll1	tubulin tyrosine ligase-like 1	0.65	0.00001
Leprel4	leprecan-like 4	0.65	0.00178
Adhfe1	alcohol dehydrogenase, iron containing, 1	0.65	0.00118
Fah	fumarylacetoacetate hydrolase	0.65	0.00130
Entpd4	ectonucleoside triphosphate diphosphohydrolase 4	0.66	0.04073
Dpyd	dihydropyrimidine dehydrogenase	0.66	0.00043
Fbln1	fibulin 1	0.66	0.01377

Gene Symbol	Gene Description	Fold Change	*P* Value
Efnb3	ephrin B3	0.66	0.00088
Stom	stomatin	0.66	0.02360
Lipe	lipase, hormone sensitive	0.67	0.00956
Cdh5	cadherin 5	0.67	0.04511
Bcl2l11	BCL2-like 11 (apoptosis facilitator)	0.67	0.00215
Adra1b	adrenergic receptor, alpha 1b	0.67	0.00369
Slc22a3	solute carrier family 22 (organic cation transporter), member 3	0.67	0.00014
AI464131	expressed sequence AI464131	0.68	0.00596
Fgf9	fibroblast growth factor 9	0.68	0.00002
Snrpn/Snurf	small nuclear ribonucleoprotein N upstream reading frame	0.68	0.00089
Smco4	single-pass membrane protein with coiled-coil domains 4	0.68	0.00035
Khdrbs3	KH domain containing, RNA binding, signal transduction associated 3	0.68	0.00147
Tmem 164	transmembrane protein 164	0.69	0.02876

Table 5

Top 50 most significantly downregulated genes in cardiomyocytes of male cardiomyocyte-specific GPER KO vs. WT mice

Gene Symbol	Gene Description	Fold Change	*P* Value
Dmd	dystrophin, muscular dystrophy	0.21	0.00012
Amy1	amylase 1, salivary	0.26	0.00000
Gpr116	G protein-coupled receptor 116	0.39	0.00162
Pah	phenylalanine hydroxylase	0.43	0.00832
Aldob	aldolase B, fructose-bisphosphate	0.44	0.00000
Gpcpd1	glycerophosphocholine phosphodiesterase GDE1 homolog	0.47	0.00307
Ppp2r3a	protein phosphatase 2, regulatory subunit B", alpha	0.49	0.00002
Pfkfb1	6-phosphofructo-2-kinase/fructose-2,6-biphosphatase 1	0.50	0.00003
Pde7a	phosphodiesterase 7A	0.50	0.01219
Fbln1	fibulin 1	0.53	0.00075
Gdap10	ganglioside-induced differentiation-associated-protein 10	0.54	0.03215
Iigp1	interferon inducible GTPase 1	0.55	0.00188
Ankrd32	ankyrin repeat domain 32	0.55	0.03600
Pdgfd	platelet-derived growth factor, D polypeptide	0.56	0.00006
2310040G07Rik	RIKEN cDNA 2310040G07 gene	0.56	0.01438
Exoc2	exocyst complex component 2	0.56	0.00000
Luc712	LUC7-like 2 (S. cerevisiae)	0.57	0.03289
Kcnj3	potassium inwardly-rectifying channel, subfamily J, member 3	0.57	0.00332
Fabp4	fatty acid binding protein 4, adipocyte	0.58	0.00018
Ano 10	anoctamin 10	0.58	0.00000
Prrg 1	proline rich Gla (G-carboxyglutamic acid) 1	0.58	0.00031
Dpyd	dihydropyrimidine dehydrogenase	0.58	0.00003
Gpr22	G protein-coupled receptor 22	0.58	0.00771
Btnl9	butyrophilin-like 9	0.59	0.00825
Ddx3y	DEAD (Asp-Glu-Ala-Asp) box polypeptide 3, Y-linked	0.59	0.02995
Ets1	E26 avian leukemia oncogene 1,5' domain	0.59	0.03764
B230214O09Rik	RIKEN cDNA B23 0214O09 gene	0.59	0.00219
Cyr61	cysteine rich protein 61	0.59	0.01297
D7Ertd715e	DNA segment, Chr 7, ERATO Doi 715, expressed	0.59	0.01290
Wif1	Wnt inhibitory factor 1	0.59	0.01242
Cav2	caveolin 2	0.60	0.04897
Kcnd2	potassium voltage-gated channel, Shal-related family, member 2	0.60	0.00045
Il15	interleukin 15	0.61	0.03395
Gbp6	guanylate binding protein 6	0.61	0.00999
Etl4	enhancer trap locus 4	0.61	0.00752
Acot1	acyl-CoA thioesterase 1	0.61	0.02195
Ttll1	tubulin tyrosine ligase-like 1	0.61	0.00000

Gene Symbol	Gene Description	Fold Change	*P* Value
Eltd1	EGF, latrophilin seven transmembrane domain containing 1	0.61	0.01848
Btnl9	butyrophilin-like 9	0.61	0.02541
Dcakd	dephospho-CoA kinase domain containing	0.62	0.00000
Cyyr1	cysteine and tyrosine-rich protein 1	0.62	0.02812
Zbtb20	zinc finger and BTB domain containing 20	0.62	0.04300
Hnrnpa3	heterogeneous nuclear ribonucleoprotein A3	0.63	0.02435
Cyr61	cysteine rich protein 61	0.63	0.01999
Ube2b	ubiquitin-conjugating enzyme E2B	0.63	0.03951
Trdn	triadin	0.63	0.00371
1810011O10Rik	RIKEN cDNA 1810011O10 gene	0.64	0.01249
Ssbp2	single-stranded DNA binding protein 2	0.64	0.00017
Tmod3	tropomodulin 3	0.64	0.04622
PggtIb	protein geranylgeranyltransferase type I, beta subunit	0.64	0.03485

Table 6

Summary of IPA in cardiomyocytes of female cardiomyocyte-specific GPER KO vs. WT mice

Top Canonical Pathways		
Name	p-value	Overlap
Cardiomyocyte Differentiation via BMP Receptors	2.38E-03	10.0 % (2/20)
Maturity Onset Diabetes of Young (MODY) Signaling	2.62E-03	9.5% (2/21)
Epoxysqualene Biosynthesis	7.26E-03	50.0 % (1/2)
Antigen Presentation Pathway	8.00E-03	5.4% 2/37
Trehalose Degradation II (Trehalase)	1.09E-02	33.3% (1/3)
Top Diseases and Disorders		
Name	p-value	#Molecules
Psychological Disorders	1.84E-02 - 1.30E-04	9
Neurological Disease	2.16E-02 - 1.94E-04	18
Skeletal and Muscular Disorders	1.84E-02 - 1.94E-04	15
Hematological Disease	2.16E-02 - 5.76E-04	8
Immunological Disease	2.16E-02 - 5.76E-04	7
Molecular and Cellular Functions		
Name	p-value	#Molecules
Carbohydrate Metabolism	1.71E-02 - 3.90E-05	6
Molecular Transport	1.81E-02 - 3.90E-05	11
Small Molecule Biochemistry	1.83E-02 - 3.90E-05	14
Cell Death and Survival	2.16E-02 - 9.80E-05	27
Cellular Development	1.81E-02 - 1.12E-04	19
Physiological System Development and Function		
Name	p-value	#Molecules
Embryonic Development	2.13E-02 - 9.80E-05	12
Hematological System Development and Function	1.81E-02 - 1.12E-04	8
Behavior	7.26E-03 - 1.30E-04	3
Nervous System Development and Function	1.81E-02 - 1.30E-04	15
Tissue Development	1.81E-02 - 1.30E-04	15
Cardiotoxicity		
Name	p-value	#Molecules
Cardiac Arrhythmia	1.97E-01 - 9.33E-04	4
Cardiac Congestive Cardiac Failure	3.64E-03 - 3.64E-03	1
Heart Failure	2.36E-01 - 3.64E-03	2
Cardiac Transformation	7.26E-03 - 7.26E-03	1
Cardiac Hypertrophy	4.09E-01 - 8.95E-03	5

Table 7

Summary of IP A in cardiomyocytes of male cardiomyocyte-specific GPER KO vs. WT mice

Top Canonical Pathways		
Name	p-value	Overlap
Dendritic Cell Maturation	3.24E-04	3.4% 6/177
B Cell Development	6.61E-04	9.1% 3/33
Antigen Presentation Pathway	9.27E-04	8.1% 3/37
Autoimmune Thyroid Disease Signaling	1.86E-03	6.4 % 3/47
Graft-versus-Host Disease Signaling	1.98E-03	6.2 % 3/48
Top Diseases and Disorders		
Name	p-value	#Molecules
Neurological Disease	7.99E-03 - 6.59E-10	42
Endocrine System Disorders	5.67E-03 - 4.82E-09	37
Gastrointestinal Disease	7.77E-03 - 4.82E-09	44
Metabolic Disease	5.19E-03 - 4.82E-09	28
Immunological Disease	7.99E-03 - 6.33E-09	32
Molecular and Cellular Functions		
Name	p-value	#Molecules
Cell Death and Survival	7.99E-03 - 4.95E-07	49
Cellular Movement	7.52E-03 - 8.19E-07	31
Cell-To-Cell Signaling and Interaction	7.79E-03 - 3.12E-05	31
Cellular Assembly and Organization	7.99E-03 - 7.97E-05	30
Cell Morphology	7.79E-03 - 8.66E-05	29
Physiological System Development and Function		
Name	p-value	#Molecules
Immune Cell Trafficking	7.52E-03 - 8.19E-07	21
Hematological System Development and Function	7.79E-03 - 1.29E-06	27
Endocrine System Development and Function	5.19E-03 - 1.45E-04	7
Cardiovascular System Development and Function	5.75E-03 - 1.59E-04	19
Organ Morphology	5.19E-03 - 1.59E-04	5
Cardiotoxicity		
Name	p-value	#Molecules
Cardiac Hypertrophy	1.17E-01 - 2.08E-06	11
Congenital Heart Anomaly	1.42E-03 - 1.42E-03	2
Cardiac Infarction	3.43E-03 - 1.46E-03	5
Cardiac Necrosis/Cell Death	2.61E-01 - 1.83E-03	6
Cardiac Arrhythmia	2.68E-01 - 3.13E-03	5